Desalination and Water Treatment
www.deswater.com
doi: 10.1080/19443994.2015.1082510

57 (2016) 16843–16854
August

Taylor & Francis
Taylor & Francis Group

Equilibrium and kinetic studies on the adsorption of humic acid onto cellulose and powdered activated carbon

Nikita Tawanda Tavengwa[a,b,*], Luke Chimuka[b], Lilian Tichagwa[a,c]

[a]*Department of Pure and Applied Chemistry, University of Fort Hare, Alice Campus, Private Bag X1314, Alice 5700, South Africa, email: nikita.tavengwa@students.wits.ac.za (N.T. Tavengwa)*
[b]*Molecular Sciences Institute, School of Chemistry, University of Witwatersrand, Private Bag 3, Johannesburg 2050, South Africa*
[c]*Department of Polymer Science & Engineering, Harare Institute of Technology, P.O. Box BE 277, Belvedere, Harare, Zimbabwe*

Received 18 March 2015; Accepted 7 August 2015

ABSTRACT

The removal of humic acid (HA) from aqueous solution onto cellulose (CE) and powdered activated carbon (PAC) was investigated in a batch adsorption system as a function of pH, sorbent mass and contact time. The optimum conditions for HA uptake by CE were 2–3, 50 mg and 30 min, respectively. For PAC, they were 2, 50 mg and 30 min, respectively. PAC and CE sorbents were characterized by Fourier transform infrared spectroscopy and scanning electron microscopy. The kinetic adsorption data was analysed on the basis of Lagergren pseudo-first-order, pseudo-second-order, Bangham and the interparticle diffusion models. The Lagergren pseudo-first-order fitted the kinetic data best. Experimental sorption data were fitted on different adsorption isotherm models, and it was established that the fitting followed the order: Langmuir > Freundlich > Temkin > Dubinin–Radushkevich (D–R). According to the Langmuir isotherm models, the maximum adsorption capacities of CE and PAC for HA were 89.3 and 30.4 mg g^{-1}, respectively.

Keywords: Humic acid; Cellulose; Activated carbon; Kinetics; Adsorption; Modelling

1. Introduction

Humic acids (HAs) are complex products of decaying vegetation, and are usually aromatic and acidic in nature [1]. The presence of HA in water resources has been of concern in water supply and there is considerable practical interest to minimize the presence of these compounds in drinking water [2]. Humic substances adversely affect water quality in several ways, causing undesirable colour and taste [3]. The presence of HAs in water does not directly cause toxicity but can (after disinfection process) result in the production of undesirable and dangerous post reactive molecules called disinfectant by-products [4]. HA can react with chlorine during water treatment producing trihalomethanes (THMs) which are carcinogenic substances [5]. The United States Environmental Protection Agency (USEPA) commends a maximum contamination level of below 80 μg L^{-1} for THMs in drinking water [6]. THMs can be reduced by removing humic materials prior to chlorination [7]. HAs have many organic functional groups that provide abundant potential binding sites for various pollutants, which also influences contaminants' dispersion and mobility in the environment. HA elimination from aqueous solution is of great significance. Furthermore,

*Corresponding author.

HA is thought to be one of the major reasons for the transport of metal ions in the environment [8]. There are several methods used to remove HA in natural water, including electrocoagulation [9], membrane technologies [10], photocatalytic degradation on Ti-modified silica [11] and adsorption [12,13]. Among these methods, adsorption is generally regarded as a promising method, and has been extensively studied for the removal of humic substances.

Activated carbon (AC) is a widely used adsorbent for industrial water treatment as well as municipal water purification [1,14]. It is a highly porous amorphous solid consisting of microcrystallites with a graphite lattice structure. The preparation involves carbonization where a carbonaceous material is exposed to elevated temperatures of between 400 and 600˚C in an oxygen-deficient atmosphere. This is followed by activation, where carbonized particles are subjected to a stream of CO_2 at high temperatures. AC can be in powdered (PAC) or granulated (GAC) form which is a form of AC with a high surface area and adsorbs many toxic compounds. Since it is from a non-renewable source, there is need for an alternative. AC is also expensive [15,16] which is becoming unaffordable to poor municipalities in developing countries in Asia and Africa. The fouling rate of AC adsorbent is high so the replacement rate or the regeneration efficiency is also high. Since AC is in the powdered form, it makes handling a big problem.

Cellulose (CE) was selected as a sorbent in this work because it is a natural organic compound with the formula $(C_6H_{10}O_5)_n$ and is the most abundant organic polymer on earth [17,18]. This insoluble polysaccharide consists of a linear chain of several hundreds to over ten thousands β(1 → 4) glycosidicly linked D-glucose units. CE is mainly obtained from wood pulp and cotton because structural component of plants are formed primarily from cellulose. It forms crystals (cellulose I_α) where intramolecular (O3–H → O5′ and O6 →H–O2′) and intrastrand (O6–H → O3′) hydrogen bonds hold the network flat, allowing the more hydrophobic ribbon faces to stack [19]. Each residue is oriented 180˚ to the next with the chain synthesized two residues at a time [20]. Although individual strands of cellulose are intrinsically no less hydrophilic, or no more hydrophobic, than some other soluble polysaccharides (such as amylase), this tendency to form crystals utilizing extensive intra- and intermolecular hydrogen bonding makes it completely insoluble in normal aqueous solutions.

In the light of the above-mentioned negative effects of the HA's presence in water, this research aims to study the effects of parameters such as initial pH, sorbent mass (PAC and CE), contact time and initial concentration on adsorption efficiency of HA by cellulose and powdered activated carbon (PAC). Kinetic and adsorption modelling studies were done to determine the rate limiting steps and gain some mechanistic information.

2. Materials and methods

2.1. Chemicals and reagents

HA was bought from Sigma Aldrich (Steinheim, Germany). The pH of the KNO_3 solution was adjusted with NaOH and HCl. Cellulose was bought from Merck (Darmastadt, Germany), while AC was obtained from Sigma Aldrich (Steinheim, Germany). All other chemicals used were of analytical reagent grade from Merck (Darmastadt, Germany), and were used without further purification.

Perkin Elmer UV–vis Lamda 25 spectrophotometer (MA, USA) was used for the analysis of humic acid concentration. For mechanical agitation, a Wisecube Fuzzy Control System from Wisd Laboratory Instruments was used at 155 rpm at a fixed temperature of 37˚C. A Rotofix 32 A Centrifuge from Hettich Lab Technology (Tuttlingen, Germany) was used to separate the HA solution from the sorbent, and was set at 3,000 rpm. Fourier transform infrared spectroscopy (FTIR) analysis was done as KBr disc on a Perkin Elmer Paragon 2000 FTIR spectrophotometer (Shelton, USA) in the range 400–4,000 cm^{-1}. For morphological feature studies of the sorbents, scanning electron microscopy (SEM), FEI Quanta 200 at 5 kV was used. Ultrapure water (Milli-Q, MA, USA) was used in all experiments. A 766 Calimatic pH meter, equipped with a Shott N61 pH electrode from Knick (Berlin, Germany) was used to measure pH.

2.2. Preparation of HA stock and standard solutions

HA (0.25 g) was transferred to a 250-mL volumetric flask where 3.3 mL of 1 M NaOH was added to necessitate its complete dissolution. The flask was shaken then topped up to the mark with distilled water. The stock solution was stored at 25˚C in a dark cupboard when not in use. Standard solutions (5–250 mg L^{-1}) were then prepared in 100-mL volumetric flasks from the HA stock solution. The calibration curve for the absorption of HA gave a good linear curve with a correlation coefficient (R^2) value of 0.999, and was confidently used for quantification. The molar absorption coefficient of HA is equal to the gradient of the calibration curve, and was determined to be 0.0053 L mol^{-1} cm^{-1}.

2.3. Determination of physicochemical properties of the sorbents

2.3.1. Determination of moisture content

Moisture content of PAC and CE was determined by weighing 3 g of the sorbent into a crucible. This was placed in the oven and heated for 3 h at a constant temperature of 120°C. The sample was then removed and put into a desiccator in order to prevent moisture uptake from the atmosphere before the sample was reweighed. This procedure was repeated until a constant weight was obtained. The difference in the mass constituted the amount of moisture content of the adsorbent.

2.3.2. Determination of loss of mass on ignition

The determination of loss of mass on ignition was done by weighing 5 g of the PAC adsorbent and put inside a furnace at constant temperature of 600°C for 1.5 h. After heating, the sample was removed and put in a desiccator to cool. The residual product was then weighed, and the difference in mass represented the mass of organic material.

2.3.3. Determination of point of zero charge (pH_{pzc})

For the point of zero charge (pH_{pzc}) determination, 0.1 mol L^{-1} KNO_3 solution was prepared, and its initial pH (pH_i) was adjusted to between 1 and 12 using NaOH and HCl in different test tubes. A 12 mL aliquot of pH-adjusted KNO_3 and 100 mg of adsorbent were then mixed in a test tube and placed in a Wisecube shaker at 37°C set at 155 rpm. After 24 h, the mixture was centrifuged for 5 min at 3,000 rpm, and the final pH (pH_f) of the solution was measured. This was done for each pH.

2.4. Batch adsorption

HA solution was transferred to a 100-mL conical flask were 50 mg of the sorbent (PAC or CE) was placed. The mechanical agitation of the mixture in a Wisecube Fuzzy Control System for maximum sorption of HAs was ensured through a steady shaking of 155 rpm. At too high stirring speed, the shaking became violent and the HA sorption was affected by the generation of air bubbles. The HA-adsorbent mixture was then allowed to equilibrate for preset HA initial pH (2–11). Mass of sorbent (10–500 mg), agitation time (5–120 min) and initial HA concentration (20–250 mg L^{-1}) were also optimized. After sorption, the mixture was centrifuged for 5 min before the supernatant was analysed for HA using a Perkin Elmer UV–vis spectrophotometer set at a wavelength of 465 nm which was a wavelength used by other researchers [21,22]. All experiments were done in triplicate at 37°C by varying one parameter and fixing the rest. The influence of adsorption parameters was evaluated by calculating the adsorption capacity, q (mg g^{-1}) defined as mass of substrate bound on a gram of adsorbent (Eq. (1)).

$$q = \frac{(C_o - C_e)V}{m} \tag{1}$$

where C_o (mg L^{-1}) is the initial concentration, and C_e (mg L^{-1}) represents the final equilibrium concentration after adsorption. V (L) is the volume of the sample solution and m (g) the mass of the adsorbent.

2.5. Kinetic model estimation

The kinetics of adsorption is important as it controls process efficiency. Kinetic studies were carried out to determine the rate and mechanism of reactions. In the present investigation, pseudo-first-order, pseudo-second-order, intraparticle diffusion and the Bangham's models were studied to determine the rate-limiting step of HA sorption onto surfaces of CE and PAC sorbents across the liquid phase.

A simple kinetic analysis of adsorption can be expressed by a pseudo-first-order equation (Lagergren equation) [23], as shown in Eq. (2):

$$\log(q_e - q_t) = \log q_e - \frac{k_1}{2.303}t \tag{2}$$

where q_e and q_t are the loading capacities (in mg g^{-1}) at equilibrium and at time t (min), respectively. The rate constant k_1 (min^{-1}) was determined from the slope of a plot of $\log(q_e - q_t)$ vs. t.

For the pseudo-second-order chemisorption kinetic, the rate equation can be expressed as [24]:

$$\frac{t}{q_t} = \frac{1}{k_2 q_e^2} + \frac{1}{q_e}t \tag{3}$$

where k_2 is the rate constant of pseudo-second-order (g mg min^{-1}) obtained from the intercept of the plot of t/q_t vs. t. The other terms are as previously defined.

To examine the diffusion mechanism of the adsorption process, the Weber and Morris intraparticle diffusion model [25] was applied to analyse the kinetic results:

$$q_t = k_{id} t^{1/2} + C \tag{4}$$

where k_{id} (mg g^{-1} min$^{-0.5}$) is the diffusion rate constant, and C reflects the boundary layer effect. If intraparticle diffusion is involved, then the plot q_t vs. $t^{1/2}$ gives a straight line with the slope k_{id} and the intercept, C.

The slowest step in the adsorption process can be determined by plotting the kinetic data with Bangham equation [26] which is expressed as:

$$\log \log \frac{C_o}{C_o - q_t m} = \log \frac{k_o}{2.303V} + \alpha \log t \tag{5}$$

where C_o is the initial concentration of the solution (mg L^{-1}), V (L) is the volume of the solution, m is the mass of the adsorbent used per litre of the solution (g L^{-1}), q_t (mg g^{-1}) is the amount of the adsorbent retained at time t (min), and α and k_o are constants.

2.6. Adsorption modelling

Sorption equilibrium is usually described by isotherm equations whose parameters express the surface properties and affinity of the sorbent at a fixed temperature and pH [27]. Distribution of HA between the liquid phase and the solid phase (PAC and CE) can be described by several isotherm models, four of which were considered in this study; Langmuir, Freundlich, Dubinin–Radushkevich and Temkin isotherms.

The Langmuir isotherm assumes that the highest adsorption happens when a saturated monolayer of solute molecules exists on the adsorbent surface (homogenous system) [28].

$$\frac{1}{q_e} = \frac{1}{q_m b C_e} + \frac{1}{q_m} \tag{6}$$

where q_e is the adsorbed amount (mg g^{-1}) of HA and C_e is the equilibrium concentration in solution (mg L^{-1}). q_m is the monolayer adsorption capacity (mg g^{-1}) and b is the constant related to the free energy of adsorption (L mg^{-1}) obtained from the plot of Eq. (6). The essential features of Langmuir adsorption isotherm parameter can be used to predict the affinity between the sorbate and sorbent using a dimensionless constant called separation factor or equilibrium parameter (R_L), which is expressed by the following relationship:

$$R_L = \frac{1}{(1 + bC_o)} \tag{7}$$

where b (L mg^{-1}) is the Langmuir constant and C_o (mg L^{-1}) is the initial concentration. The value of R_L provides information as to whether the adsorption is irreversible ($R_L = 0$), favourable ($0 < R_L < 1$), linearly favourable ($R_L = 1$) or unfavourable ($R_L > 1$).

The Freundlich isotherm model is an empirical relationship describing the adsorption of solutes from a liquid to a solid surface, and assumes that different sites with several adsorption energies are involved, and is represented by Eq. (8) [29].

$$\log q_e = \log k_F + \frac{1}{n} \log C_e \tag{8}$$

where q_e is the amount of HA adsorbed per unit mass of adsorbent (mg g^{-1}) and C_e is the concentration of HA at equilibrium (mg L^{-1}). k_F (L mg^{-1}) roughly shows the adsorption capacity and $1/n$ represents the adsorption intensity.

Dubinin–Radushkevich isotherm does not assume a homogeneous surface or constant sorption potential. It is commonly applied in the following form [30]:

$$\ln q_e = \ln q_m - \beta_D \varepsilon^2 \tag{9}$$

where q_m (mg g^{-1}) is maximum adsorption capacity and β_D (mol^2 J^{-2}) is the activity coefficient associated with adsorption energy. The Polanyi potential (ε) is given in Eq. (10), R (J mo1^{-1} K^{-1}) is the universal gas constant and T (K) is temperature. β_D and q_m are calculated from the slope and intercept of the plot $\ln q_e$ vs. ε^2, respectively. The mean adsorption energy, E (kJ mol^{-1}), is obtained from Eq. (11) and its value determines the type of adsorption process as physical ($E < 8$ kJ mol^{-1}) or chemical ($E > 16$ kJ mol^{-1}).

$$\varepsilon = RT \ln\left(1 + \frac{1}{C_e}\right) \tag{10}$$

$$E = \frac{1}{\sqrt{(2B_D)}} \tag{11}$$

By ignoring the extremely low and large values of concentration, the Temkin isotherm model assumes that the heat of adsorption of all molecules in a layer would decrease linearly rather than logarithmically with coverage. Its derivation is characterized by a uniform distribution of binding energies up to some maximum binding energy, which was determined by plotting the quantity sorbed q_e against $\ln C_e$. The constants were determined from the slope and intercept of Eq. (12) [31].

$$q_e = \frac{RT}{b_T} \ln A_T + \frac{RT}{b_T} \ln C_e \quad (12)$$

where A_T (L g^{-1}) and b_T are the Temkin isotherm equilibrium binding constants.

3. Results and discussion

3.1. Characterization studies

HA can be characterized as a loose assembly of aromatic polymer of varying acidity and reactivity with a hypothetical structure as shown in Fig. 1. Table 1 summarizes some important physicochemical characteristics of the sorbents (PAC and CE).

Moisture content is an essential component of any sorbent material which determines the ability of the sorbent to hold the moisture. Moisture content depends on many factors such as the composition of the sorbent, thus the different values for CE and PAC which were 6.7 and 7.0%, respectively. A material with high moisture content has a high porosity and the active groups are spaced further apart from each other [33].

FTIR spectra of CE, HA, and CE–HA complex were investigated to determine the functional groups which participated in the formation of the complex (Fig. 2). The shaded bands are included to highlight the several differences in the three spectra. For HA, the prominent peak at 3,439.03 cm^{-1} confirmed that it had hydroxyl groups. This band, due to –OH, was one of the functional groups used in the adsorption of HA to the CE adsorbent. The peak at 1,611.57 cm^{-1} signified the presence of double bonds. The bond at 1,622.18 cm^{-1} suggested the presence of double bonds in CE. HA itself have been found to be a good sorbent for different analytes such as metal ion contaminants [34] because of its functional groups. Previous FTIR studies have shown absorbance wavelengths at 3,416, 2,916, 1,638, 1,417, 1,323, 1,161, 1,046 and 895 cm^{-1} to be associated with native cellulose [35,36]. The FTIR spectrum of CE–HA was basically an overlap of the CE's and HA's. There were bonds in HA which were not present in its spectrum but appeared in that of the CE–HA complex (1,430 and 1,300 cm^{-1}). However, bands at 900, 825, 700, 450 and 440 cm^{-1} were strongly present in the pure HA spectrum but their intensity

Table 1
Physicochemical properties of the sorbents

Sorbent property	Sorbent	
	CE	PAC
Colour	White	Black
Specific gravity (g cm^{-3})	1.62	0.8–2.1
Moisture content (%)	6.7	7.0
Loss of mass on ignition (%)	–	8.9
Point of zero charge (pH$_{pzc}$)	7.8	9.2
BET surface area (m^2 g^{-1})	102	834

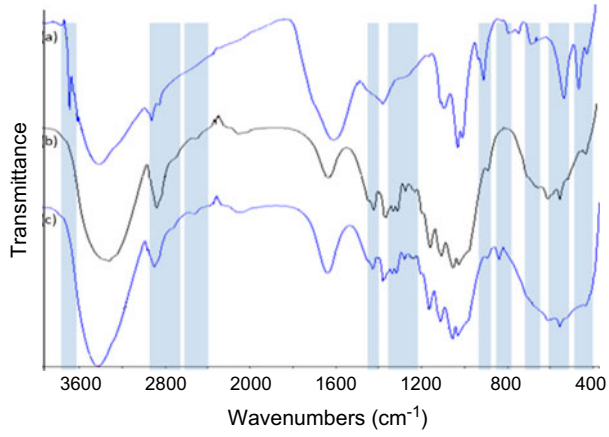

Fig. 2. FTIR spectra of (a) HA, (b) CE and (c) CE–HA complex (shaded regions highlight the differences).

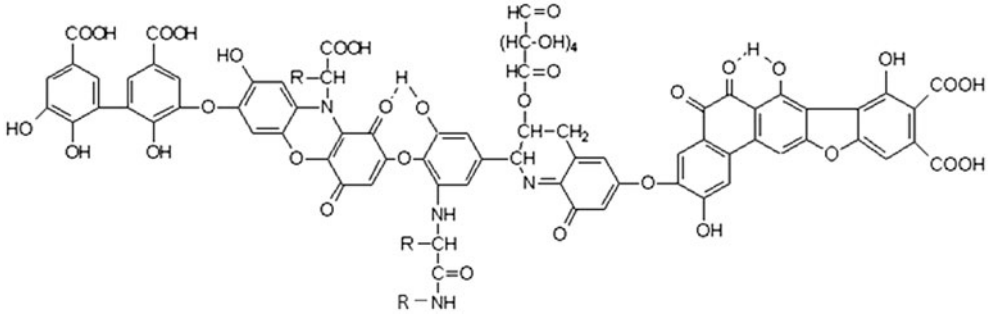

Fig. 1. A model structure of HA [32].

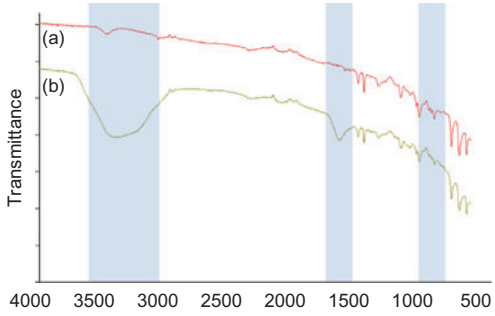

Fig. 3. FTIR spectra of (a) PAC and (B) PAC–HA complex (shaded regions highlight the differences).

were greatly diminished in the spectrum of the complex. The absorption band of the carboxyl group at 1,700 cm^{-1} for CE remained considerably strong after reaction with HA indicating that only part of the carboxyl group participated in the bonding process.

Fig. 3 shows an FTIR spectrum of PAC with no detail in the functional group region. However, after adsorption of HA from a solution, several adsorption bands appeared both in the functional group and the fingerprint regions. The presence of the band around 3,350 cm^{-1} was indicative of the hydroxyl ions from water where the HA was spiked. The C=C bond of the HA was observed in the PAC–HA complex and was an indication of bonding between PAC and HA.

The surface physical morphology of the sorbents was evaluated by SEM. Both the SEM images showed surfaces that were not smooth (Fig. 4). This is an important surface feature, as the roughness of the sorbent meant high available surface area for HA adsorption. The pores on the surface enhanced the mass transfer of the HA from the bulk solution to the pores of the sorbent.

3.2. Effect of pH and point of zero charge (pH_{pzc})

The surfaces of the sorbents (CE and PAC) and HA were affected differently by basic and acidic conditions, as such, different adsorption values were observed at different pH values. Solution pH strongly influences the surface charge of the adsorbing material, degree of ionization process of HA molecules, and this parameter was investigated in the pH range of 2–11 (Fig. 5). For the determination of point of zero charge (pH_{pzc}), a plot of ΔpH vs. pH_i was used (Fig. 6). The pH value where ΔpH = 0 was the point of zero charge (pH_{pzc}), which is the pH at which the total number of positive and negative charges on its surface becomes zero was found to be 9.2 for CE. It has been found that the pH_{pzc} of chitosan, which is structurally related to cellulose, was 6.6 [2]. At pH < 9.2, the surface of the cellulose was taken as positive, and the HA, which is negatively charged due to its $pH_{pzc} \approx 2$ [37] was adsorbed strongly by electrostatic attraction. It can be seen from the hypothetical structure of HA that the –COOH, –OH and –NH groups are negative centre carriers. The increase in the number of negatively charged sites on cellulose beyond pH_{pzc} resulted in electrostatic repulsion with the HA molecules and lower adsorption capacities were thus recorded. The same pH trend was found by Song et al. [38] who modified graphene oxide nanosheets with cyclodextrin in an investigation of HA removal.

Effect of pH on HA sorption onto PAC followed a similar trend to that of CE (Fig. 5). HA molecules generally gain excess negative surface charge as the pH is increased due to deprotonation, firstly by the carboxylic groups at pH values of 4–6, followed by the dissociation of phenolic groups at higher pH [39,40]. From Fig. 6, the pH_{pzc} of PAC was found to be 7.8. In another research, it was observed that pH_{pzc} of AC cloth in KNO_3 aqueous solutions was at pH 7.0 [41]. pH_{pzc} of 7.98 of

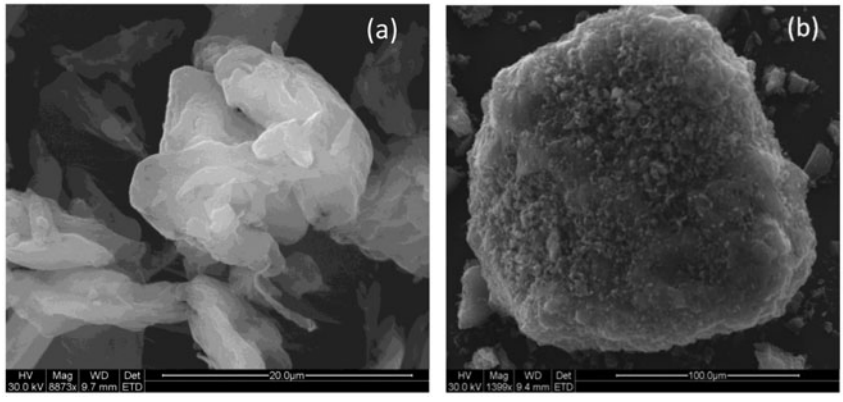

Fig. 4. SEM micrography of (a) CE and (b) PAC.

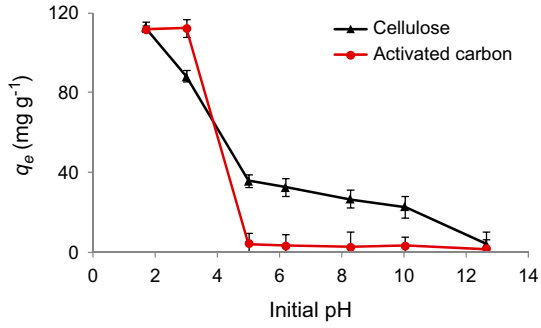

Fig. 5. Effect of initial pH on the adsorption of HA on PAC and cellulose (n = 3). (Sample volume = 25 mL, HA concentration = 200 mg L^{-1}, contact time = 50 min, sorbent (CE and PAC) weight = 50 mg, temperature = 37˚C.)

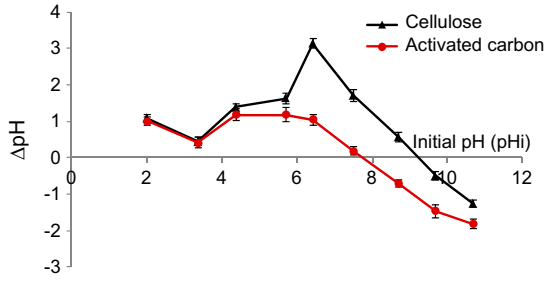

Fig. 6. Determination of point of zero charge (pH_{pzc}) of HA adsorbed on PAC and cellulose by varying the inital pH (n = 3).

pyrolytically prepared AC from *Fagopyrum esculentum* Moench was obtained by Kibami et al. [42]. Just like in this study, Diaz-Flores et al. [43] used an anionic molecule, 2,4-dichlorophenoxyacetic acid, for sorption unto AC cloth and reported a pH_{pzc} of 9.41 and the maximum sorption they recorded was at pH 2–3.

3.3. Effect of sobent mass

The effect of the sobent mass on the removal of HA from aqueous solution was investigated by varying the mass of the adsorbent (CE and PAC) from 10 to 500 mg (Fig. 7). It is expected that an increase in the mass of adsorbent should yield a corresponding increase in the amount of HA adsorbed onto the surface of the adsorbent since there will be more adsorption sites available. Therefore, competition for binding sites between molecules of the adsorbate decreased with increase in mass of the adsorbent. With increasing adsorbent dose, the removal efficiency increased and corresponding adsorbed quantity per unit mass decreased. The best mass was found to be 50 mg for both sorbents and was used in subsequent experiments.

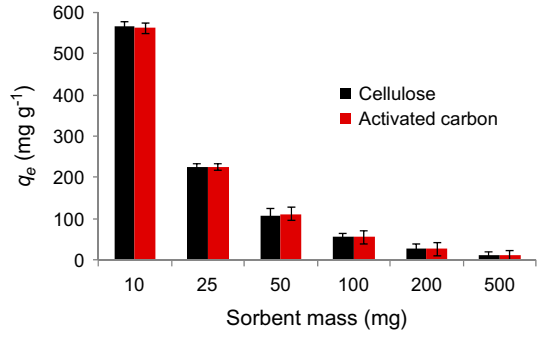

Fig. 7. Effect of sorbent mass on the adsorption of HA on PAC and cellulose (n = 3). (Sample volume = 25 mL, HA concentration = 200 mg L^{-1}, contact time = 50 min, temperature = 37˚C.)

3.4. Effect of contact time

The contact time between HA adsorbate and the sorbent (CE and PAC) is of great importance in the design of a sorption systems and large-scale applications. Therefore, time-dependent experiments were conducted in the range of 5–120 min at 37˚C (Fig. 8). As can be seen, the maximum sorption was achieved after 30 min for both sorbents. This was an indication that the sorption of HA on both sorbents was a fast mass transfer. The fast sorption rate could have been due to a great availability of surface area/binding sites on the sorbents during the initial stages. Generally, HA molecules will bind to all the active sites until they are fully occupied. Hence, with time, fewer active sites are available leading to a reduction in the amount of HA adsorbed.

3.5. Effect of initial concentration

Initial concentration is an important parameter which may provide an important driving force to overcome all mass transfer resistance of adsorbate

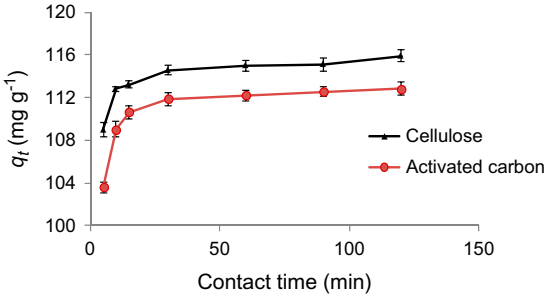

Fig. 8. Effect of contact time of HA adsobed on PAC and cellulose (n = 3). (Sample pH 4, sample volume = 25 mL, HA concentration = 200 mg L^{-1}, sorbent (CE and PAC) weight = 50 mg, temperature = 37˚C.)

between the aqueous and solid phases. It influences the rate at which adsorbate molecules move from the bulk solution to the adsorbent surface [27]. Increasing initial concentration enhanced the adsorption capacity of HA (Fig. 9). This trend was also observed by Moussavi et al. [4]. The almost linear dependency might have been due to the unsaturation of binding sites of CE and PAC which resulted in an increase in the HA removal. As shown in Fig. 9, when the initial concentration of aqueous HA solution was changed from 20 to 250 mg L^{-1}, the absolute amount of HA adsorbed per unit mass of cellulose and PAC also increased.

3.6. Kinetic modelling

The rate constants of pseudo-first-order (k_1) were found to be 0.029 and 0.030 min^{-1} for HA adsorption onto CE and AC, respectively (Table 2). The comparison of q_e values from experimental work ($q_{e,exp}$ = 109.4 and 111.8 mg g^{-1}) of this study and the calculated ones ($q_{e,cal}$ = 5.06 and 5.32 mg g^{-1}) of pseudo-first-order kinetic model showed a large difference. This did not show the suitability of this model. Furthermore, the degree of linearity for these kinetic model plots was judged from the value of the correlation coefficients. The correlation coefficients (R^2) were 0.895 and 0.868 for CE and AC, respectively. Therefore, the fitting of the experimental data to the pseudo-first-order was not good. The $q_{e,exp}$ (109.4 and 111.8 mg g^{-1}) and the $q_{e,cal}$ (113.6 and 116.3 mg g^{-1}) values from the pseudo-second-order kinetic model were close to each other. In addition, the calculated correlation coefficients (R^2) were both unity (for CE and AC) for this model (Fig. 10(a) and Table 2). These findings suggested that the pseudo-second-order adsorption mechanism was predominant and that the overall rate of the HA adsorption process was most likely to be controlled by the chemisorption process for both sorbents. The intraparticle diffusion is only rate-limiting step if the plot passes through the origin. Alternatively, both the external diffusion and the intraparticle diffusion contribute to the whole adsorption process when the straight line deviates from the origin. The larger C values (105.7 and 110.1) indicated the greater effect of the boundary layer on diffusion. Since the plots are not totally linear and do not pass through their respective origins, intraparticle diffusion could not be the phenomena at play. As a rule of thumb, if equilibrium is achieved within 3 h, the process is usually kinetic controlled and above 24 h, it is diffusion controlled [44]. Bangham's equation was used to evaluate whether the adsorption was pore-diffusion controlled. Plots of log log$[C_o/(C_o - q_t m)]$ vs. log t for the sorption of HA onto CE and AC gave correlation values of 0.820 and 0.899, respectively (Fig. 10(d) and Table 2) which confirmed that the adsorption was pore-diffusion controlled. The constants α and k_o are obtained from Fig. 10(d) and are given in Table 2 as 0.094 and 0.056 for CE, and 0.093 and 0.066 for AC.

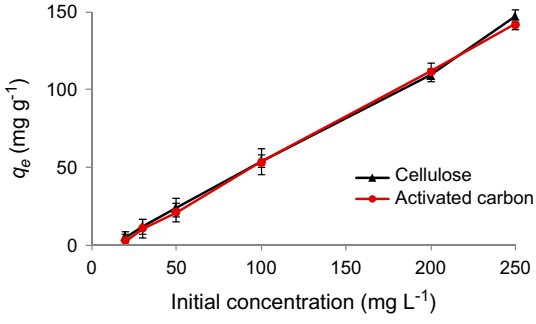

Fig. 9. Effect of initial concentration of HA adsorbed on cellulose and PAC (n = 3). (Sample pH 4, sample volume = 25 mL, contact time = 50 min, sorbent (CE and PAC) weight = 50 mg, temperature = 37°C.)

Table 2
Pseudo-first-order, pseudo-second-order, intraparticle model, and the Bangham's model constants for the adsorption of HA onto CE and PAC

Adsorption model	Modelling parameter	CE	PAC
Pseudo-first-order	q_m (mg g^{-1})	5.06	5.32
	k_1 (min^{-1})	0.029	0.030
	R^2	0.895	0.868
	RMSE	46	48
Pseudo-second-order	q_e (mg g^{-1})	113.6	116.3
	k_2 (g mg^{-1} min^{-1})	0.022	0.023
	R^2	1	1
Intraparticle model	k_{id} (mg g^{-1} $min^{-0.5}$)	0.76	0.59
	C	105.7	110.1
	R^2	0.604	0.702
	RMSE	1.88	2.01
Bangham's model	α	0.094	0.093
	k_o	0.056	0.066
	R^2	0.820	0.899

For the pseudo-first and pseudo-second-orders, the residual root mean square errors (RMSE) of the adsorption capacities were determined (Eq. (13)). RMSE represents the match between the experimental data and the calculated data obtained from plotting the isotherm and is defined as [45]:

$$\mathrm{RMSE} = \sqrt{\frac{1}{n-2}\sum_{i=1}^{N}(q_{e,exp} - q_{e,cal})^2} \quad (13)$$

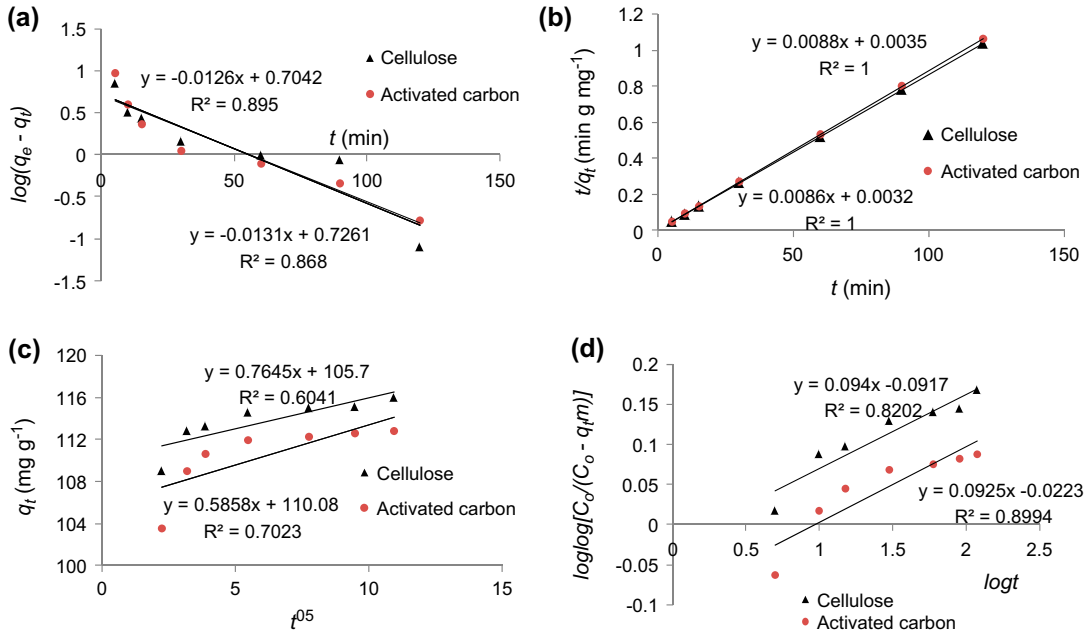

Fig. 10. Kinetic models of (a) pseudo-first-order, (b) pseudo-second-order, (c) intraparticle model and (d) Bangham's plot.

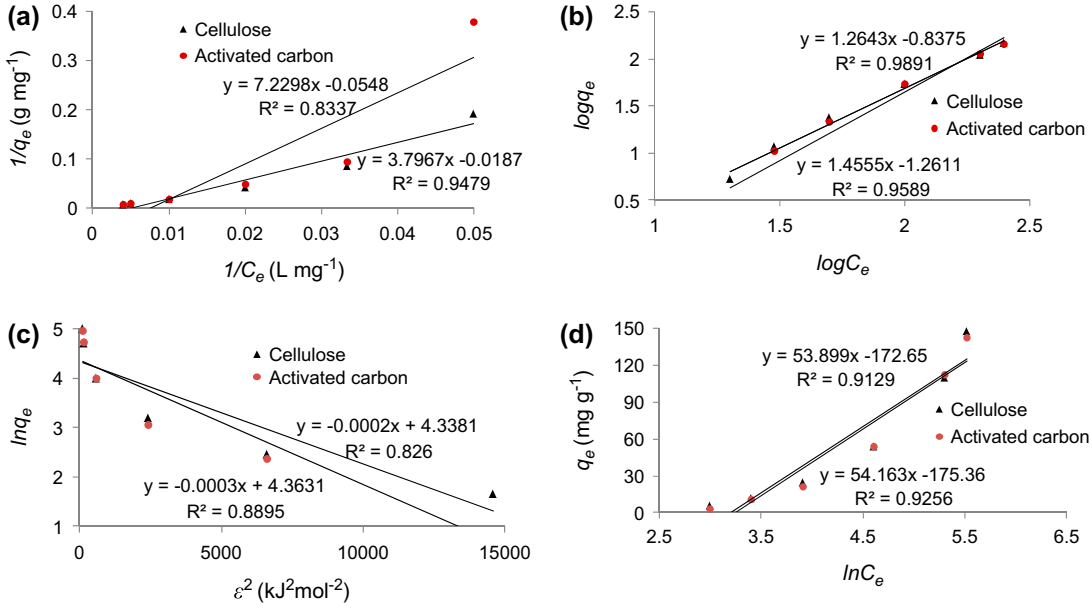

Fig. 11. Adsorption models (a) Langmuir, (b) Freundlich, (c) Dubinin–Radushkevich and (d) Temkin isotherms.

where n is the number of data points. If the estimated data are very similar to the experimental data, then the RMSE value is small. The smaller RMSE values obtained from the pseudo-second-order (1.88 and 2.01 for the CE and PAC, respectively) further emphasizing the better fitting of this model to the kinetic data.

3.7. Adsorption modelling

Linear plots of the investigated models are shown in Fig. 11 and a summary of the theoretical parameters of adsorption isotherms along with regression coefficients are listed in Table 3. Langmuir isotherm parameter fits for HA adsorption on CE and AC

Table 3
Equilibrium isotherm parameters

Adsorption model	Modelling parameter	CE	PAC
Langumuir	q_m (mg g^{-1})	89.3	30.4
	b (L mg^{-1})	0.0076	0.0049
	R_L	0.397	0.504
	R^2	0.8337	0.9479
Freundlich	k_F (L mg^{-1})	4.13	10.9
	n	0.791	0.69
	R^2	0.9891	0.9589
Dubinin–Radushkevich	B_D (mol^2 kJ^{-2})	0.0002	0.0003
	q_m (mg g^{-1})	128	131
	E (kJ mol^{-1})	50	41
	R^2	0.826	0.8895
Temkin	b_T (J mol^{-1})	27.6	27.5
	A_T (L g^{-1})	24.6	25.5
	R^2	0.9129	0.9256

yielded isotherms that were in good agreement with observed behaviour with $R^2 > 0.83$ and $R^2 > 0.94$ as correlation coefficients, respectively. Since R_L values for CE and AC, 0.397 and 0.504, respectively, fell in the range of 0–1, the sorption of HA onto these sorbents was concluded to be favourable. The adsorption capacities of HA onto CE and AC were found to be 89.3 and 30.4 mg g^{-1}. These values were close to the experimental values obtained in this study (109.4 and 111.8 mg g^{-1}). The HA adsorption capacity on CE and AC were compared to other similar sorbents (Table 4). Though the correlation coefficients for the Freundlich models were high for CE and AC ($R^2 > 0.98$ and $R^2 > 0.95$, respectively), the Freundlich constants (n) were <1 (0.79 and 0.69 for CE and AC, respectively) indicating the unsuitability of this model. Moreso, the Freundlich k_F values for CE and AC (4.1 and 10.9 L g^{-1}, respectively) which approximates the adsorption capacities were lower than the experimental values. For Dubinin–Radushkevich model, values of E between 1 and 8 kJ mol^{-1} indicate physical adsorption; those higher than 8 kJ mol^{-1} indicate that the process is chemical in nature [46]. The values obtained in this experiment were 50 kJ mol^{-1} for the cellulose and 41 kJ mol^{-1} for the AC; therefore, the type of HA adsorption on the adsorbent materials was likely to be chemisorption. Linear plots for Temkin adsorption isotherm (Fig. 11(c)), which refer to

Table 4
Comparison with other similar sorbents used for HA removal

Sorbent	q_{max} (mg g^{-1})	pH	Refs.
Carbon based sorbent			
Single-walled carbon nanotubes	33.2	4	[4]
Fly ash	10.7	3	[47]
Activated carbon	97.4	≈2	[48]
Activated carbon	30.4	2	This work
Glucose based sorbent			
Chitosan-coated granules	0.41	<6	[2]
Cyclodextrin modified graphene oxide nanosheets	32.6	5	[38]
Chitosan	3,300	≈7.3[a]	[49]
Chitin	189	≈7.3[a]	[49]
Crosslinked chitosan-epichlorohydrin beads	44.8	6	[50]
Cellulose	89.3	2	This work

[a]Not optimized but chosen to simulate the environment of the upper intestinal tract.

chemisorption of an adsorbate onto the adsorbent, fitted quite well with correlation coefficients >0.91 and >0.92, for CE and AC, respectively.

4. Conclusions

In this study, cellulose and PAC were found to have good adsorption capacity for HA from an aqueous solution. These sorbents can be used for HA removal before chlorination to avoid the formation of cancerous trihalomethanes. The high sorption of HA at low pH values can also be attributed to its precipitation from solution. From the initial concentration data, the Langmuir adsorption isotherms provided the best fitting model which indicated that a chemisorption mechanism was mainly involved in the adsorption of HA onto the two sorbents. From the effect of contact time, kinetics of sorption followed the pseudo-second-order model, further emphasizing the chemisorption mechanism.

References

[1] M.A. Ferro-García, J. Rivera-Utrilla, I. Bautista-Toledo, C. Moreno-Castilla, Adsorption of humic substances on activated carbon from aqueous solutions and their effect on the removal of Cr(III) ions, Langmuir 14 (1998) 1880–1886.

[2] X. Zhang, R. Bai, Mechanisms and kinetics of humic acid adsorption onto chitosan-coated granules, J. Colloid Interface Sci. 264 (2003) 30–38.

[3] M.A. Zulfikar, Effect of temperature on adsorption of humic acid from peat water onto pyrophyllite, IJCEBS 1 (2013) 88–90.

[4] S.P. Moussavi, M.H. Ehrampoush, A.H. Mahvi, M. Ahmadian, S. Rahimi, Adsorption of humic acid from aqueous solution on single-walled carbon nanotubes, Asian J. Chem. 25 (2013) 5319–5324.

[5] M.Y. Chang, R.S. Juang, Adsorption of tannic acid, humic acid, and dyes from water using the composite of chitosan and activated clay, J. Colloid Interface Sci. 278 (2004) 18–25.

[6] J. Kim, Y. Chung, D. Shin, M. Kim, Y. Lee, Y. Lim, D. Lee, Chlorination by-products in surface water treatment process, Desalination 151 (2002) 1–9.

[7] S.E. Manahan, Fundamentals of Environmental Chemistry, Lewis Publishers, Boca Raton, Florida, 1993.

[8] M.A. Rashid, Geochemistry of Marine Humic Compounds, Springer-Verlag, New York, 1985, p. 62.

[9] F. Ulu, S. Barışçı, M. Kobya, H. Särkkä, M. Sillanpää, Removal of humic substances by electrocoagulation (EC) process and characterization of floc size growth mechanism under optimum conditions, Sep. Purif. Technol. 133 (2014) 246–253.

[10] A. Mehrparvar, A. Rahimpour, M. Jahanshahi, Modified ultrafiltration membranes for humic acid removal, J. Taiwan Inst. Chem. Eng. 45 (2014) 275–282.

[11] T. Moriguchi, K. Yano, M. Tahara, K. Yaguchi, Metal-modified silica adsorbents for removal of humic substances in water, J. Colloid Interface Sci. 283 (2005) 300–310.

[12] J. Wang, L. Bi, Y. Ji, H. Ma, X. Yin, Removal of humic acid from aqueous solution by magnetically separable polyaniline: Adsorption behavior and mechanism, J. Colloid Interface Sci. 430 (2014) 140–146.

[13] X. Qin, F. Liu, G. Wang, G. Huang, Adsorption of humic acid from aqueous solution by hematite: Effects of pH and ionic strength, Environ. Earth Sci. 73 (2015) 4011–4017.

[14] F.S. Baker, C.E. Miller, A.J. Repik, E.D. Tolles, Activated carbon, Kirk-Othmer Encyc. Chem. Technol. 4 (1992) 1015–1037.

[15] D. Mohan, K.P. Singh, Single- and multi-component adsorption of cadmium and zinc using activated carbon derived from bagasse—An agricultural waste, Water Res. 36 (2002) 2304–2318.

[16] J.H. Potgieter, S.O. Bada, S.S. Potgieter-Vermaak, Adsorptive removal of various phenols from water by South African coal fly ash, Water SA 35 (2009) 89–96.

[17] C. Satgé, B. Verneuil, P. Branland, R. Granet, P. Krausz, J. Rozier, C. Petit, Rapid homogeneous esterification of cellulose induced by microwave irradiation, Carbohydr. Polym. 49 (2002) 373–376.

[18] J. Credou, T. Berthelot, Cellulose: From biocompatible to bioactive material, J. Mater. Chem. B 2 (2014) 4767–4788.

[19] A. Isogai, R.H. Atalla, Preparation of cellulose-chitosan polymer blends, Carbohyd. Polym. 19 (1992) 25–28.

[20] R.A. Festucci-Buselli, W.C. Otoni, C.P. Joshi, Structure, organization, and functions of cellulose synthase complexes in higher plants, Braz. J. Plant Physiol. 19 (2007) 1–13.

[21] L.F. Zara, A.H. Rosa, I.A.S. Toscano, J.C. Rocha, A structural conformation study of aquatic humic acid, J. Braz. Chem. Soc. 17 (2006) 1014–1019.

[22] S.S. Fong, L. Seng, W.N. Chong, J. Asing, M.F.M. Nor, A.S.M. Pauzan, Characterization of the coal derived humic acids from Mukah, Sarawak as soil conditioner, J. Braz. Chem. Soc. 17 (2006) 582–587.

[23] S. Lagergren, Zur theorie der sogenannten adsorption geloster stoffe (About the theory of so-called adsorption soluble substances), Kungliga Svenska Vetenskapsakademiens, Handlingar 24 (1898) 1–39.

[24] Y.S. Ho, G. McKay, D.A.J Wase, C.F. Foster, Study of the sorption of divalent metal ions on to peat, Adsorp, Sci. Technol. 18 (2000) 639–650.

[25] W.J. Weber, J.C. Morris, Kinetics of adsorption on carbon from solution, Sanit. Eng. Div. Am. Soc. Civ. Eng. 89 (1963) 31–40.

[26] C. Aharoni, S. Sideman, E. Hoffer, Adsorption of phosphate ions by colloid ion-coated alumina, J. Chem. Technol. Biotechnol. 29 (1979) 404–412.

[27] J. Wu, H.Q. Yu, Biosorption of 2,4-dichlorophenol from aqueous solution by Phanerochaete chrysosporium biomass: Isotherms, kinetics and thermodynamics, J. Hazard. Mater. 137 (2006) 498–508.

[28] I. Langmuir, The constitution and fundamental properties of solids and liquids. Part I. Solids, J. Am. Chem. Soc. 38 (1916) 2221–2295.

[29] H.M.F. Freundlich, Über die adsorption in lösungen (Over the adsorption in solution), Zeitschrift für Physikalische Chemie 57 (1906) 385–470.
[30] M.M. Dubinin, The potential theory of adsorption of gases and vapors for adsorbents with energetically nonuniform surfaces, Chem. Rev. 60 (1960) 235–241.
[31] M.J. Tempkin, V. Pyozhev, Kinetics of ammonia synthesis on promoted iron catalyst, Acta Physicochim. USSR 12 (1940) 327–352.
[32] F.J. Stevenson, Humus Chemistry. Genesis, Composition, Reactions, John Wiley and Sons, New York, NY, 1982.
[33] B.A. Shah, A.V. Shah, P.M. Shah, Sorption isotherms and column separation of Cu(II) and Zn(II) using ortho substituted benzoic acid chelating resins, Arch. Appl. Sci. Res. 3 (2011) 327–341.
[34] J.H. Chen, J.C. Ni, Q.L. Liu, S.X. Li, Adsorption behavior of Cd(II) ions on humic acid-immobilized sodium alginate and hydroxyl ethyl cellulose blending porous composite membrane adsorbent, Desalination 285 (2012) 54–61.
[35] S.Y. Oh, D.I. Yoo, Y. Shin, H.C. Kim, H.Y. Kim, Y.S. Chung, W.H. Park, J.H. Youk, Crystalline structure analysis of cellulose treated with sodium hydroxide and carbon dioxide by means of X-ray diffraction and FTIR spectroscopy, Carbohydr. Res. 340 (2005) 2376–2391.
[36] C.F. Liu, R.C. Sun, A.P. Zhang, J.L. Ren, Z.C. Geng, Structural and thermal characterization of sugarcane bagasse cellulose succinates prepared in ionic liquid, Polym. Degrad. Stab. 91 (2006) 3040–3047.
[37] W.L. Yan, R. Bai, Adsorption of lead and humic acid on chitosan hydrogel beads, Water Res. 39 (2005) 688–698.
[38] W. Song, D. Shao, S. Lu, X. Wang, Simultaneous removal of uranium and humic acid by cyclodextrin modified graphene oxide nanosheets, Sci. China Chem. 57 (2014) 1291–1299.
[39] A.A.M. Daifullah, B.S. Girgis, H.M.H. Gad, A study of the factors affecting the removal of humic acid by activated carbon prepared from biomass material, Colloids Surf., A 235 (2004) 1–10.
[40] A. Jada, R.A. Ait Akbour, J. Douch, Surface charge and adsorption from water onto quartz sand of humic acid, Chemosphere 64 (2006) 1287–1295.
[41] B.M. Babić, S.K. Milonjić, M.J. Polovina, B.V. Kaludierović, Point of zero charge and intrinsic equilibrium constants of activated carbon cloth, Carbon 37 (1999) 477–481.
[42] D. Kibami, C. Pongener, K.S. Rao, D. Sinha, Preparation and characterization of activated carbon from *Fagopyrum esculentum* Moench by HNO_3 and H_3PO_4 chemical activation, Der Chem. Sin. 5 (2014) 46–55.
[43] P.E. Diaz-Flores, R. Leyva-Ramos, J.R. Rangel-Mendez, M.M. Ortiz, R.M. Guerrero-Coronado, J. Mendoza-Barron, Adsorption of 2,4-dichlorophenoxyacetic acid from aqueous solution on activated carbon cloth, J. Environ. Eng. Manage. 16 (2006) 249–257.
[44] Y.S. Ho, J.C.Y. Ng, G. McKay, Kinetics of pollutant sorption by biosorbents: Review, Sep. Purif. Rev. 29 (2000) 189–232.
[45] D.C. Montgomery, Design and Analysis of Experiments, John Wiley & Sons, New York, NY, 2001.
[46] M.S. Onyango, Y. Kojima, A. Kumar, D. Kuchar, M. Kubota, H. Matsuda, Uptake of fluoride by Al^{3+} pretreated low-silica synthetic zeolites: Adsorption equilibrium and rate studies, Sep. Sci. Technol. 41 (2006) 683–704.
[47] S. Wang, Z.H. Zhu, Humic acid adsorption on fly ash and its derived unburned carbon, J. Colloid Interface Sci. 315 (2007) 41–46.
[48] M.S. Rauthula, V.C. Srivastava, Studies on adsorption/desorption of nitrobenzene and humic acid onto/from activated carbon, Chem. Eng. J. 168 (2011) 35–43.
[49] J. Chen, C. Yeh, L. Wang, T. Liou, C. Shen, C. Liu, Chitosan, the marine functional food, is a potent adsorbent of humic acid, Mar. Drugs 9 (2011) 2488–2498.
[50] N.W.S. Wan, M.A.K.M. Hanafiah, S.S. Yong, Adsorption of humic acid from aqueous solutions on cross-linked chitosan-epichlorohydrin beads: Kinetics and isotherm studies, Colloids Surf., B 65 (2008) 18–24.